Journal of the Physical Society of Japan
Vol. 71, No. 10, October, 2002, pp. 2414–2426

Two-Time Correlation Function of a Two-Dimensional Quantal Rotator in a Colored Noise

Yoko SUZUKI* and Yoshitaka TANIMURA

Institute for Molecular Science, Myodaiji, Okazaki 444-8585

(Received April 17, 2002)

We study an absorption spectrum of a two-dimensional rotator coupled to a colored harmonic-oscillator bath. The absorption spectrum is analytically calculated from the generating functional of a reduced density matrix element for the rotator degrees of freedom. In the previous letter [J. Phys. Soc. Jpn. **70** (2001) 1167], the analysis of spectrum is limited to a white noise case. In this paper, we extend our theory to a colored noise case. We present the spectra for different temperatures, damping strength, and the correlation time of the noise. For a weakly damped rotator, at low temperatures, the spectra are sensitive to the system dynamics that is determined by the quantization of the rotational motion. Such a quantized rotational motion depends on the noise effects. Hence we observe the peak shifts by the noise correlation time. For a strongly damped rotator, we find the bimodal spectrum in the slow modulation case. One of the peaks is caused by the effect of the colored noise, which dose not appear in the case of the white noise. This peak is related to a librational motion induced by the coupling between the system and the bath oscillators with the near zero frequencies.

KEYWORDS: two-dimensional rotator, dissipative system, path integral, correlation function
DOI: 10.1143/JPSJ.71.2414

1. Introduction

In physics and chemistry, rotational motions in a dissipative environment is as important as translational and vibrational motions. The rotational relaxation plays an important role in dielectric absorption[1)] and dispersion, the infrared (IR), far-IR or rotational-Raman spectra[2,3)] of solutions. For example, a role of the rotational relaxation is observed in Fourier transform infrared spectroscopy of methane molecules embedded in parahydrogen crystals.[4)]

Theoretically, the dissipative effects are investigated by means of computer simulations or by employing model systems that can by solved analytically. Computer simulations[5–8)] provide reasonable results; however, it is computationally expensive to study relaxation effects by them, especially, in a quantum case, since they require large-scale long-time calculations and they often complicate the understanding of the problem. Simpler models that include the necessary complexity to address dissipation make possible to compensate these disadvantages. In this paper, we investigate quantum dynamics of a damped rotator system modeled by a free rotator coupled to a harmonic oscillator heat-bath based on an analytical expression of two-time correlation functions. The translational and vibrational motions in the dissipative environments are commonly modeled by a Brownian oscillator model, which consists of a system coupled to a harmonic oscillator bath.[9–12)] For the rotational motion, one faces the complication of how to formulate a coupling scheme that dose not ignore the periodicity of angle variable. In order to solve this problem, there are two ways to describe the system: the energy level representation and the coordinate representation. In the former, we describe the rotator system in terms of the discrete energy level arising from the quantization of the rotational degree of freedom with a cyclic boundary condition.[13–15)] The effects of dissipation are introduced by artificially adopting the life time of these energy levels. In the coordinate representation, the rotator system is expressed in terms of the angle coordinate satisfying the cyclic boundary condition.[16,17)] The dissipation is defined as the coupling between this angular coordinate and the environment. Such a description allows us the clear establishment of the relation between the quantum model and the phenomenological classical model. A model Hamiltonian is then denoted by the two-dimensional rotator system coupled to the environment represented by an ensemble of harmonic oscillators, which satisfies the cyclic boundary condition of the rotator system. In this paper, we use the latter representation to investigate the quantum rotator in a Gaussian–Markovian noise bath. The effects of the environment, *e.g.*, temperature and noise, can be studied with the absorption spectra that are calculated from the generating functional. In the previous letter,[18)] we present the absorption spectra related to the two-time correlation function of the damped rotator for a Gaussian-white noise bath. In this paper, we present the calculational details of the correlation functions and the analysis of the spectra for a Gaussian–Markovian bath.

The heat-bath acts as a noise source, which induces a fluctuation in the system through the system-bath interaction. In characterizing the time scale of the noise correlation plays an important role. In many cases, *e.g.*, molecular collision or lattice vibration, the noise correlation time is required to be so short that the approximation of completely uncorrelated fluctuations is valid. In such a case, the noise is assumed to be the Gaussian-white noise characterized by the noise correlation function $\gamma(t) = 2\gamma\delta(t)$, where γ implies the system-bath coupling strength. In liquids, however, where the motions of the bath molecules have a similar time scale as the motions of the system, this approximation is invalid and a more elaborate model is necessary, which accounts for the finite correlation of the system and the bath motions. One of examples is the Gaussian–Markovian noise characterized by the noise correlation function $\gamma(t) = \gamma\omega_D e^{-\omega_D t}$, in which ω_D corresponds to the inverse correlation time of the noise. It is noted that the Gaussian-white noise is the zero limit of the noise correlation time in the Gaussian–Markovian noise;

*E-mail: youko@ims.ac.jp

i.e., $\omega_D \to \infty$ leads $\gamma\omega_D e^{-\omega_D t}$ to $2\gamma\delta(t)$.

In §2, we define the model Hamiltonian that reduces the Langevin equation in the classical limit. The derivation of the Langevin equation is given in Appendix A. In §3, we give the analytical expression of the generating functional in the case of the Gaussian–Markovian noise. The calculational details are shown in Appendices B and C. In §4, the two-time correlation function is derived from the generating functional. The numerical results and their discussion are presented in §5. Section 6 is devoted to the conclusion.

2. Response Function for Optical Processes

The Hamiltonian of the multi-dimensional rotator coupled to the heat bath is written as

$$\hat{H} = \frac{L^2}{2\mu} + \sum_i \left[\frac{\hat{p}_i^2}{2m_i} + \frac{m_i\omega_i^2}{2}\left(\hat{q}_i - \frac{c_i\theta}{m_i\omega_i^2}\right)^2 \right]. \tag{2.1}$$

Here, L, θ, and μ are the angular momentum defined by $L \equiv (\hbar/i)\partial/\partial\theta$, the angular coordinate, and the moment of inertia, respectively. The coordinate, conjugate momentum, mass, and frequency of the ith bath oscillator are given by $\hat{q}_i$, $\hat{p}_i$, m_i, and ω_i. The bath operators $\hat{q}_i$ and $\hat{p}_i$ commutate with the system operators θ and L. Note that original rotational symmetry of the rotator recovers and the angular coordinate is $-\pi \le \theta < \pi$ with $\theta = -\pi$ and $\theta = \pi$ identified after tracing out the bath degrees of freedom owing to the properties of the Gaussian integration. We choose the form eq. (2.1) in order to have the Langevin equation for the rotational motion

$$\mu\ddot{\theta}(t) + \int_{t_I}^{t} \mathrm{d}t'\eta(t-t')\dot{\theta}(t') = R(t), \tag{2.2}$$

$$\langle R(t)\rangle_I = 0, \tag{2.3}$$

$$\langle R(t)R(t')\rangle_I = \frac{1}{\beta}\eta(t-t'), \tag{2.4}$$

in the classical limit. Here $\eta(t)$ is a friction kernel describing the dissipative influence of the heat bath, $R(t)$ is the random torque that satisfies eqs. (2.3) and (2.4) and $\langle\cdots\rangle_I$ is the expectation value for the thermal equilibrium initial state at the initial time $t = t_I$, as is shown in Appendix A. We consider the optical response of the rigid rotator. The linear absorption spectrum is calculated from the Fourier transformation of the two-time correlation function of the dipole moment. Since the dipole moment is expressed as $d = d_0\cos\theta$, the spectrum is written as[19)]

$$\sigma(\omega) = \mathrm{Im}\left[\frac{\mathrm{i}}{\hbar} d_0^2 \int_0^\infty \mathrm{d}t e^{\mathrm{i}\omega t}\langle[\cos\theta(t), \cos\theta(0)]\rangle\right]. \tag{2.5}$$

Here, $\cos\theta(t) \equiv e^{\mathrm{i}\hat{H}t/\hbar}\cos\theta e^{-\mathrm{i}\hat{H}t/\hbar}$ and $\langle\cdots\rangle$ means the expectation value of "$\cdots$" defined by $\langle\cdots\rangle = \mathrm{Tr}(e^{-\beta\hat{H}}\cdots)/\mathrm{Tr}\, e^{-\beta\hat{H}}$ in which β is the inverse temperature. Note that eq. (2.5) corresponds to the third-order off-resonant Raman response by the replacement of d with the polarizability α.

3. Generating Functional

In order to calculate the correlation function of $\cos\theta$, we introduce an artificial source $\mathcal{K}_\alpha(t)$ ($\alpha = 1, 2, 3$) coupled to $\cos\theta$ and define the generating functional $Z[\mathcal{K}]$ as follows,

$$Z[\mathcal{K}] = \mathrm{Tr}\left(\hat{\rho}_I^{\mathcal{K}_3}\hat{U}_{\mathcal{K}_2}^\dagger(\infty, t_I)\hat{U}_{\mathcal{K}_1}(\infty, t_I)\right), \tag{3.1}$$

where

$$\hat{U}_{\mathcal{K}_\alpha}(\infty, t_I) = \mathrm{T}_t\left(e^{-\frac{\mathrm{i}}{\hbar}\int_{t_I}^{\infty}\mathrm{d}t\left(\hat{H} - \mathcal{K}_\alpha(t)\cos\theta\right)}\right), \tag{3.2}$$

and

$$\hat{\rho}_I^{\mathcal{K}_3} = \mathrm{T}_\tau\left(e^{-\frac{1}{\hbar}\int_0^{\beta\hbar}\mathrm{d}\tau\left(\hat{H} - \frac{\mathrm{i}}{\hbar}\mathcal{K}_3(\tau)\cos\theta\right)}\right). \tag{3.3}$$

Here, $\hat{\rho}_I^{\mathcal{K}_3=0}$ gives an equilibrium distribution at the initial time t_I and τ is the imaginary time parameter with $0 \le \tau \le \beta\hbar$. The symbol T_t (T_τ) stands for the real (imaginary) time ordering operator. We represent the function in the two-real-time paths by the suffixes $\alpha = 1, 2$ and the imaginary one by $\alpha = 3$, respectively.

The two-time correlation function of $\cos\theta$ is evaluated from the generating functional as

$$\langle \mathrm{T}_C\cos\theta(t_0)\cos\theta(t_1)\rangle = \frac{1}{Z[\mathcal{K}=0]}\left(\frac{\hbar}{\mathrm{i}}\right)^2 \frac{\delta^2 Z[\mathcal{K}]}{\delta_C\mathcal{K}(t_0)\delta_C\mathcal{K}(t_1)}\bigg|_{\mathcal{K}=0}. \tag{3.4}$$

Here, the index C implies the contour time path that starts from t_I to ∞ along the real path (C_1), returns to t_I (C_2) and goes to $t_I - \mathrm{i}\beta\hbar$ parallel to the imaginary axis (C_3).[20,21)] The operator T_C and the function $\delta_C(t)$ are the time-ordering operator and the δ-function on the contour time path, respectively. The functional differentiation $\delta/\delta_C\mathcal{K}(t)$ means $\delta/\delta\mathcal{K}_1(t)$, $-\delta/\delta\mathcal{K}_2(t)$, and $(\hbar/\mathrm{i})\delta/\delta\mathcal{K}_3(t)$ for $t \in C_1$, $t \in C_2$, and $t \in C_3$.

In order to evaluate $Z[\mathcal{K}]$, we consider the unitary transformation which was utilized in the analysis of a free particle coupled to a harmonic-oscillator bath.[22)] We set $\hat{y}_i \equiv m_i\omega_i^2\hat{q}_i/c_i$, $\hat{p}_{yi} \equiv c_i\hat{p}_i/(m_i\omega_i^2)$, $\mu_i \equiv c_i^2/(m_i\omega_i^4)$ and $r_i \equiv \mu_i/\mu'$ with $\mu' \equiv \mu + \sum_j \mu_j$. Then the unitary operator is expressed as

$$\hat{X} = \exp\left(-\frac{\mathrm{i}}{\hbar}\theta\sum_i \hat{p}_{yi}\right)\exp\left(\frac{\mathrm{i}}{\hbar}\sum_i r_i L\hat{y}_i\right). \tag{3.5}$$

By the unitary transformation $\hat{X}$, the Hamiltonian is separated into the free rotator part and the heat bath part as

$$\tilde{\hat{H}} \equiv \hat{X}^\dagger\hat{H}\hat{X} = \tilde{H}_S(L) + \tilde{H}_B(\hat{p}_{yi}, \hat{y}_i), \tag{3.6}$$

where

$$\tilde{H}_S(L) = \frac{1}{2\mu'}L^2, \tag{3.7}$$

and

$$\tilde{H}_B(\hat{p}_{yi}, \hat{y}_i) = \frac{1}{2\mu}\left(\sum_i \hat{p}_{yi}\right)^2 + \sum_i\left(\frac{\hat{p}_{yi}{}^2}{2\mu_i} + \frac{1}{2}\mu_i\omega_i^2\hat{y}_i{}^2\right). \tag{3.8}$$

According to eq. (B·13) in Appendix B, the two-time correlation function eq. (3.4) is written as

$$\langle \mathrm{T}_C \cos\theta(t_0)\cos\theta(t_1)\rangle = \sum_{a_0=\pm1}\sum_{a_1=\pm1} \frac{Z_S[J]Z_B[J]}{2^2 Z_S[J=0]Z_B[J=0]}\bigg|_{J(s)=\hbar(a_0\delta_C(s-t_0)+a_1\delta_C(s-t_1))}. \tag{3.9}$$

Here, $Z_S[J]$ and $Z_B[J]$ are the generating functionals for the Hamiltonian $\tilde{H}_S - J(t)\theta$ and $\tilde{H}_B + J(t)\sum_i r_i\hat{y}_i$, respectively, and are given by

$$Z_S[J] = \sum_{l=-\infty}^{\infty} \delta_{0,R_J} \exp\left(-\frac{\mathrm{i}}{\hbar}\int_C \mathrm{d}t\tilde{H}_S(L)\right)\bigg|_{L=\hbar l+\int_{t_I(C)}^{t}\mathrm{d}sJ(s)}, \tag{3.10}$$

$$Z_B[J] = \mathrm{Tr}_B\left[\mathrm{e}^{-\frac{\mathrm{i}}{\hbar}\int_C \mathrm{d}t\left(\tilde{H}_B+J(t)\sum_i r_i\hat{y}_i\right)}\right], \tag{3.11}$$

where $R_J = \int_C \mathrm{d}tJ(t)/\hbar$ and the index C in the integral, $\int_C \mathrm{d}t$ implies the integration along the contour time path. Hereafter, we derive the product $Z_S[J]Z_B[J]$.

In the same way as in the Brownian free particle case,[10] one can obtain $Z_B[J]$. The detailed derivation of $Z_B[J]$ is shown in Appendix C. The final result is given by

$$Z_B[J] = \mathrm{e}^{\Xi[J]}\mathrm{e}^{-\Upsilon[J]}Z_B[J=0]. \tag{3.12}$$

Here, $\Upsilon[J]$ is expressed as

$$\Upsilon[J] = \frac{\mathrm{i}}{2\hbar}\int_C \mathrm{d}t\int_C \mathrm{d}t' J(t)G_{C0}(t,t')J(t'), \tag{3.13}$$

where

$$G_{C0}(t,t') = \lim_{\omega\to 0}\left[\frac{\mathrm{i}}{2\mu'\omega\sinh\frac{\omega\beta\hbar}{2}}\left(\Theta_C(t-t')\times\cos\omega\left(t-t'+\frac{\mathrm{i}\beta\hbar}{2}\right)+(t\longleftrightarrow t')\right)\right]. \tag{3.14}$$

The function $\Theta_C(t)$ in eq. (3.14) is a step function on the contour time path. The functional $\Xi[J]$ is expressed as[10]

$$\Xi[J] = \frac{\mathrm{i}}{2\hbar}\int_{t_I}^{\infty}\mathrm{d}t\int_{t_I}^{\infty}\mathrm{d}t'(2J_-(t)K_0^{(+-)}(t-t')J_+(t') + J_-(t)K_0^{(++)}(t-t')J_-(t')) + \frac{1}{\hbar}\int_{t_I}^{\infty}\mathrm{d}t\int_0^{\beta\hbar}\mathrm{d}\tau J_-(t)K_0^{(+3)}(t,\tau)J_3(\tau) - \frac{\mathrm{i}}{2\hbar}\int_0^{\beta\hbar}\mathrm{d}\tau\int_0^{\beta\hbar}\mathrm{d}\tau' J_3(\tau)K_0^{(33)}(\tau,\tau')J_3(\tau'), \tag{3.15}$$

where $K_0^{(+-)}(t)$ is denoted in the Laplace representation as

$$K_0^{(+-)}(z) = \frac{1}{\mu z^2 + \mu\hat{\gamma}(z)z}, \tag{3.16}$$

and $\hat{\gamma}(z)$ is the Laplace transform of the mass-independent damping kernel described as $\hat{\gamma}(z) \equiv \sum_i c_i^2 z/[\mu m_i\omega_i^2(z^2+\omega_i^2)]$. The functions $K_0^{(++)}(t)$, $K_0^{(+3)}(t,\tau)$, and $K_0^{(33)}(\tau)$ in eq. (3.15) are given in the Fourier-Laplace representation by

$$K_0^{(+3)}(z,\nu_n) = \frac{\mathrm{i}}{z+\nu_n}\left(K_0^{(+-)}(\nu_n) - K_0^{(+-)}(z)\right), \tag{3.17}$$

$$K_0^{(++)}(z) = \frac{1}{2}\sum_{n=-\infty}^{\infty}\mathrm{e}^{-\mathrm{i}\nu_n 0^+}\left[K_0^{(+3)}(z,\nu_n) - \left(K_0^{(+3)}(z,-\nu_n)\right)^*\right], \tag{3.18}$$

$$K_0^{(33)}(\nu_n) = \mathrm{i}K_0^{(+-)}(-\nu_n). \tag{3.19}$$

To characterize the bath, we introduce the spectral density defined formally by $I(\omega) \equiv \pi\sum_i c_i^2/(2m_i\omega_i)\delta(\omega-\omega_i)$. On the assumption of the Gaussian–Markovian dissipation, the spectral density is chosen as $I(\omega) = \mu\omega\gamma\omega_D^2/(\omega_D^2+\omega^2)$.[23,24] Here, the constants γ and ω_D relate to the mass-independent damping kernel $\gamma(t) = \int_0^\infty \mathrm{d}\omega 2I(\omega)/(\pi\mu\omega)$ by $\gamma(t) = \gamma\omega_D\mathrm{e}^{-\omega_D t}$, in which γ and ω_D correspond to the damping strength and the inverse correlation time of the noise, respectively. We note that such dissipation reduces to the Ohmic dissipation for $\omega_D \to \infty$. In the Gaussian–Markovian dissipation, $K_0^{(l,m)}$ $(l,m=\pm,3)$ is denoted in terms of

$$K_0^{(+-)}(t) = \Theta(t)\frac{1}{\mu}\left[\frac{1}{x_1-x_2}\left\{\mathrm{e}^{-x_2 t}\left(1-\frac{x_1}{\gamma}\right) - \mathrm{e}^{-x_1 t}\left(1-\frac{x_2}{\gamma}\right)\right\} + \frac{1}{\gamma}\right], \tag{3.20}$$

$$K_0^{(++)}(t) = \frac{\mathrm{i}}{\beta\hbar}\sum_{l=1}^{\infty}\frac{2\gamma\omega_D^2\mathrm{e}^{-\nu_l|t|}}{\mu\nu_l[(\nu_l^2+\gamma\omega_D)^2-\nu_l^2\omega_D^2]} + \frac{\mathrm{i}}{2\mu(x_1-x_2)}\left[\mathrm{e}^{-x_2|t|}\left(1-\frac{x_1}{\gamma}\right)\cot\left(\frac{\beta\hbar x_2}{2}\right) - \mathrm{e}^{-x_1|t|}\left(1-\frac{x_2}{\gamma}\right)\cot\left(\frac{\beta\hbar x_1}{2}\right)\right] + \frac{\mathrm{i}}{\beta\hbar}\lim_{l\to 0}\frac{\mathrm{e}^{-\mathrm{i}\omega_l 0^+}}{\mu\nu_l^2+\mu\hat{\gamma}(|\nu_l|)|\nu_l|} - \frac{\mathrm{i}}{\beta\hbar\mu\gamma}\left[\frac{1}{\omega_D}\left(1-\frac{\omega_D}{\gamma}\right)+|t|\right], \tag{3.21}$$

$$K_0^{(+3)}(t,\tau) = \frac{\mathrm{i}}{\beta\hbar}\sum_l \mathrm{e}^{-\nu_l\tau}\left(\frac{\mathrm{e}^{-\nu_l t}}{\mu\nu_l^2+\mu\hat{\gamma}(|\nu_l|)|\nu_l|} - \frac{1}{\mu}\left\{\frac{\mathrm{e}^{-\nu_l t}}{\nu_l^2-\omega_D\nu_l+\gamma\omega_D}\left(1-\frac{\omega_D-\nu_l}{\gamma}\right)+\frac{1-\mathrm{e}^{-\nu_l t}}{\gamma\nu_l} + \frac{1}{x_1-x_2}\left[\frac{\mathrm{e}^{-x_1 t}}{x_1-\nu_l}\left(1-\frac{x_2}{\gamma}\right)-\frac{\mathrm{e}^{-x_2 t}}{x_2-\nu_l}\left(1-\frac{x_1}{\gamma}\right)\right]\right\}\right), \tag{3.22}$$

and

$$K_0^{(33)}(\tau) = \frac{\mathrm{i}}{\beta\hbar}\sum_l \frac{\mathrm{e}^{-\mathrm{i}\nu_l\tau}}{\mu\nu_l^2+\mu\hat{\gamma}(|\nu_l|)|\nu_l|}, \tag{3.23}$$

where 0^+ is a positive infenitesimal quantity. Here, $J_+ \equiv (J_1+J_2)/2$, $J_- \equiv J_1 - J_2$, $\nu_l \equiv 2\pi l/(\beta\hbar)$,

$$x_{1,2} = \frac{\omega_D \pm \sqrt{\omega_D^2 - 4\gamma\omega_D}}{2}, \tag{3.24}$$

and $\Theta(t)$ is a step function.

With the help of the relation (see ref. 16, for example),

$$\sum_k \mathrm{e}^{\mathrm{i}(Ak^2+Bk)} = \sum_l \sqrt{\frac{\mathrm{i}\pi}{A}}\mathrm{e}^{-\frac{\mathrm{i}}{4A}(B+2\pi l)^2} \tag{3.25}$$

the generating functional of the rotator part $Z_S[K]$ given by eq. (3.10) is rewritten as

$$Z_S[J] = \delta_{0,R_J}\left(\frac{2\mu'\pi}{\beta\hbar^2}\right)^{\frac{1}{2}}\sum_l \mathrm{e}^{-\frac{1}{\beta\hbar^2}\left[-2\pi l\int_C \mathrm{d}s(t_I-\mathrm{i}\beta\hbar-s)J(s)+\frac{\mu'}{2}(2\pi l)^2\right]} \times \exp\left[\frac{\mathrm{i}}{2\hbar}\int_{t_I(C)}^{t_I-\mathrm{i}\beta\hbar}\mathrm{d}s\mathrm{d}s' J(s)\tilde{G}_0(s,s')J(s')\right], \tag{3.26}$$

where

$$\tilde{G}_0(s,s') = \frac{1}{\mathrm{i}\beta\hbar\mu'}\{\Theta_C(s-s')(s'-t_I)(t_I-\mathrm{i}\beta\hbar-s) + (t\longleftrightarrow t')\}. \tag{3.27}$$

To evaluate eq. (3.26), we refer to the free particle case where the coordinate, momentum, and mass are denoted by $\hat{Q}$, $\hat{P}$, and μ'. The time evolution function of a free particle is obtained by setting the oscillator frequency to zero in eq. (3-66) of ref. 25:

$$_J\langle Q_b,t_b|Q_a,t_a\rangle_J = {}_J\langle Q_b|\mathrm{T}_t\mathrm{e}^{-\frac{\mathrm{i}}{\hbar}\int_{t_a}^{t_b}\mathrm{d}t\hat{H}_0[J]}|Q_a\rangle_J = \left(\frac{\mu}{2\pi\mathrm{i}\hbar(t_b-t_a)}\right)^{\frac{1}{2}} \times \exp\left[\frac{\mathrm{i}}{\hbar}\left\{\frac{1}{2}\int_{t_a}^{t_b}\mathrm{d}s\mathrm{d}s' J(s)\tilde{G}_0(s,s';t_b,t_a)J(s') + Q_a\int_{t_a}^{t_b}\mathrm{d}s\frac{t_b-s}{t_b-t_a}J(s) + Q_b\int_{t_a}^{t_b}\mathrm{d}s\frac{s-t_a}{t_b-t_a}J(s) + \frac{\mu'}{2(t_b-t_a)}(Q_a^2-Q_b^2)\right\}\right], \tag{3.28}$$

where $\hat{H}_0[J] \equiv \hat{P}^2/(2\mu') - J(t)\hat{Q}$ and

$$\tilde{G}_0(s,s';t_b,t_a) = -\frac{1}{\mu'(t_b-t_a)}\{\Theta(s-s')(s'-t_a)(t_b-s) + (s\longleftrightarrow s')\}. \tag{3.29}$$

By using eq. (3.28), the generating functional is given by

$$Z_F[J] = \int_{-\infty}^{\infty}\mathrm{d}Q_J\langle Q|\hat{\rho}_I^S\hat{U}_S^\dagger(\infty,t_I)\hat{U}_S(\infty,t_I)|Q\rangle_J = \left(\frac{2\pi\mu'}{\beta\hbar^2}\right)^{\frac{1}{2}}\delta(R_J) \times \exp\left[\frac{\mathrm{i}}{2\hbar}\int_C \mathrm{d}s\mathrm{d}s' J(s)\tilde{G}_0(s,s';t_I,t_I)J(s')\right]. \tag{3.30}$$

Here, $\hat{\rho}_I^S$ and $\hat{U}_S^{(\dagger)}$ are defined by $\hat{\rho}_I^S \equiv \mathrm{T}_\tau\exp(-(1/\hbar)\int_0^{\beta\hbar}\mathrm{d}\tau H_0[J])$ and $\hat{U}_I^S \equiv \mathrm{T}_t\exp(-(\mathrm{i}/\hbar)\int_{t_I}^{\infty}\mathrm{d}\tau H_0[J])$. Another expression of $Z_F[J]$ is calculated from the generating functional in the harmonic oscillator system [eqs. (2.24) and (2.29) in ref. 20] by setting the oscillator frequency to zero:

$$Z_F[J] = \mathrm{e}^{\Upsilon[J]}Z_0, \tag{3.31}$$

where $Z_0 \equiv Z_F[J=0]$. Comparing eqs. (3.30) and (3.31), we obtain the following relation;

$$\delta_{0,R_J}\left(\frac{2\pi\mu'}{\beta\hbar^2}\right)^{\frac{1}{2}}\delta(0)\exp\left[\frac{\mathrm{i}}{2\hbar}\int_C \mathrm{d}s\mathrm{d}s' J(s)\tilde{G}_0(s,s')J(s')\right] = \delta_{0,R_J}\mathrm{e}^{\Upsilon[J]}Z_0. \tag{3.32}$$

Substituting eq. (3.32) into eq. (3.26), we get

$$Z_S[J] = \frac{1}{\delta(0)}\delta_{0,R_J}\mathrm{e}^{\Upsilon[J]}Z_0 \times \sum_l \mathrm{e}^{-\frac{1}{\beta\hbar^2}\left[-2\pi l\int_C \mathrm{d}s(t_I-\mathrm{i}\beta\hbar-s)J(s)+\frac{\mu'}{2}(2\pi l)^2\right]}. \tag{3.33}$$

Notice that the condition $R_J = 0$ selects transitions induced by irradiated pulses, as shown later. From eqs. (3.9), (3.12) and (3.33) we have the generating functional in the form

$$Z_S[J]Z_B[J] = \frac{1}{\delta(0)} Z_B[J=0] Z_0 \delta_{0,R_J} \mathrm{e}^{\Xi[J]} \times \sum_l \mathrm{e}^{-\frac{1}{\beta\hbar^2}\left[-2\pi l \int_C \mathrm{d}s(t_I - \mathrm{i}\beta\hbar - s)J(s) + \frac{\mu'}{2}(2\pi l)^2\right]}. \tag{3.34}$$

4. Two-Time Correlation Function

From eqs. (3.9) and (3.34), we can get an expression of the two-time correlation function. Substitution of eq. (3.34) into eq. (3.9) leads to

$$\langle \mathrm{T}_C \cos\theta(t_0)\cos\theta(t_1)\rangle = \sum_{a_0=\pm1}\sum_{a_1=\pm1} \frac{1}{2^2\Lambda}\delta_{0,R_J}\mathrm{e}^{\Xi[J]} \times \sum_l \mathrm{e}^{-\frac{1}{\beta\hbar^2}\left[-2\pi l \int_C \mathrm{d}s(t_I - \mathrm{i}\beta\hbar - s)J(s) + \frac{\mu'}{2}(2\pi l)^2\right]}\Bigg|_{J(s)=\hbar(a_0\delta(s-t_0)+a_1\delta(s-t_1))}, \tag{4.1}$$

where $\Lambda = \sum_l \mathrm{e}^{-\mu'(2\pi l)^2/(2\beta\hbar^2)}$.

The two-time correlation function is derived from eq. (4.1). For the cases, $t_0, t_1 \in C_1$ and $t_0 \in C_1, t_1 \in C_2$, we obtain

$$\begin{aligned}\langle \mathrm{T}\cos\theta(t_0)\cos\theta(t_1)\rangle &= \frac{1}{\Lambda}\sum_l \mathrm{e}^{-\frac{\mu'(2\pi l)^2}{2\beta\hbar^2}}\cosh\left(2\pi l\frac{t_0-t_1}{\beta\hbar}\right)\\ &\times\frac{1}{2}\Big(\Theta(t_0-t_1)\mathrm{e}^{\tilde{S}_{D1}(t_0-t_1)-\frac{\mathrm{i}\hbar}{2\mu}\tilde{S}_{D2}(t_0-t_1)}\\ &+\Theta(t_1-t_0)\mathrm{e}^{\tilde{S}_{D1}(t_1-t_0)-\frac{\mathrm{i}\hbar}{2\mu}\tilde{S}_{D2}(t_1-t_0)}\Big),\end{aligned} \tag{4.2}$$

$$\begin{aligned}\langle \cos\theta(t_1)\cos\theta(t_0)\rangle &= \frac{1}{\Lambda}\sum_l \mathrm{e}^{-\frac{\mu'(2\pi l)^2}{2\beta\hbar^2}}\cosh\left(2\pi l\frac{t_0-t_1}{\beta\hbar}\right)\\ &\times\frac{1}{2}\Big(\Theta(t_0-t_1)\mathrm{e}^{\tilde{S}_{D1}(t_0-t_1)+\frac{\mathrm{i}\hbar}{2\mu}\tilde{S}_{D2}(t_0-t_1)}\\ &+\Theta(t_1-t_0)\mathrm{e}^{\tilde{S}_{D1}(t_1-t_0)-\frac{\mathrm{i}\hbar}{2\mu}\tilde{S}_{D2}(t_1-t_0)}\Big),\end{aligned} \tag{4.3}$$

respectively. Here,

$$\begin{aligned}\tilde{S}_{D1}(t) &= \frac{1}{\beta\mu}\sum_{l=1}^{\infty}\frac{\mathrm{e}^{-\nu_l t}-1}{\nu_l}\frac{2\gamma\omega_D^2}{(\nu_l^2-x_1^2)(\nu_l^2-x_2^2)} - \frac{t}{\beta\mu\gamma}\\ &+\frac{\hbar}{2\mu(x_1-x_2)}\left[(\mathrm{e}^{-x_2 t}-1)\left(1-\frac{x_1}{\gamma}\right)\cot\left(\frac{\beta\hbar x_2}{2}\right)\right.\\ &\left.-(\mathrm{e}^{-x_1 t}-1)\left(1-\frac{x_2}{\gamma}\right)\cot\left(\frac{\beta\hbar x_1}{2}\right)\right],\end{aligned} \tag{4.4}$$

$$\begin{aligned}\tilde{S}_{D2}(t) &= \frac{1}{x_1-x_2}\left[(\mathrm{e}^{-x_2 t}-1)\left(1-\frac{x_1}{\gamma}\right)\right.\\ &\left.-(\mathrm{e}^{-x_1 t}-1)\left(1-\frac{x_2}{\gamma}\right)\right]\\ &= \frac{1}{\gamma}+\frac{2\mathrm{e}^{-\frac{\omega_D}{2}t}}{\omega_D\sqrt{1-4\gamma/\omega_D}}\left(1-\frac{\omega_D}{2\gamma}\right)\\ &\times\sinh\left(\frac{\omega_D t}{2}\sqrt{1-\frac{4\gamma}{\omega_D}}\right)\\ &-\frac{\mathrm{e}^{-\frac{\omega_D}{2}t}}{\gamma}\cosh\left(\frac{\omega_D t}{2}\sqrt{1-\frac{4\gamma}{\omega_D}}\right).\end{aligned} \tag{4.5}$$

From (4.2) and (4.3), the antisymmetric and symmetric correlation functions are given by

$$\begin{aligned}&\Theta(t_0-t_1)\langle[\cos\theta(t_0),\cos\theta(t_1)]\rangle\\ &= \Theta(t_0-t_1)\frac{\mathrm{i}}{\Lambda}\sum_l \mathrm{e}^{-\frac{\mu'(2\pi l)^2}{2\beta\hbar^2}}\cosh\left(2\pi l\frac{t_0-t_1}{\beta\hbar}\right),\\ &\times\mathrm{e}^{\tilde{S}_{D1}(t_0-t_1)}\sin\left(-\frac{\hbar}{2\mu}\tilde{S}_{D2}(t_0-t_1)\right),\end{aligned} \tag{4.6}$$

$$\begin{aligned}\langle\{\cos\theta(t_0),\cos\theta(t_1)\}\rangle &= \frac{1}{\Lambda}\sum_l \mathrm{e}^{-\frac{\mu'(2\pi l)^2}{2\beta\hbar^2}}\cosh\left(2\pi l\frac{t_0-t_1}{\beta\hbar}\right),\\ &\times\mathrm{e}^{\tilde{S}_{D1}(|t_0-t_1|)}\cos\left(-\frac{\hbar}{2\mu}\tilde{S}_{D2}(|t_0-t_1|)\right).\end{aligned} \tag{4.7}$$

Here, we note that $\sum_i \mu_i$ in μ' diverges for the low frequency of $I(\omega)$ as $\sum_i \mu_i = \int_{\omega_c}^{\infty}\mathrm{d}\omega 2I(\omega)/\pi\omega^3 = 2\mu\gamma[1/(\pi\omega_c) - 1/(2\omega_D)]$, where ω_c is the low frequency cut-off. The damping function $\gamma(t)$ is rewritten by using ω_c as $\gamma(t) = \int_{\omega_c}^{\infty}\mathrm{d}\omega 2I(\omega)/(\pi\mu\omega)\cos(\omega t) \sim 2\gamma\delta(t) - 2\gamma\omega_D^2 \sin(\omega_c t)/(\pi t)/(\omega_c^2+\omega_D^2)$ for large t and we find that $\gamma(t)$ has a long time tail. In the present study we focus on the motion of the rotator in a short period so that the cut-off ω_c can be regarded as being small. Equations (4.6) and (4.7) are the solution for the quantum and colored noise case. They are the main results in this paper.

In the classical limit $\hbar \to 0$, eqs. (4.6) and (4.7) become

$$\begin{aligned}&\Theta(t_0-t_1)\langle[\cos\theta(t_0),\cos\theta(t_1)]\rangle\\ &= \mathrm{i}\Theta(t_0-t_1)\left(-\frac{\hbar}{2\mu}\tilde{S}_{D2}(t_0-t_1)\right)\mathrm{e}^{\tilde{S}_{D3}(t_0-t_1)} = 0,\end{aligned} \tag{4.8}$$

$$\langle\{\cos\theta(t_0),\cos\theta(t_1)\}\rangle = \mathrm{e}^{\tilde{S}_{D3}(|t_0-t_1|)}, \tag{4.9}$$

where

$$\begin{aligned}\tilde{S}_{D3}(t) &= \frac{1}{\beta\mu}\left\{-\frac{1}{\gamma\omega_D}+\frac{1}{\gamma^2}-\frac{t}{\gamma}\right.\\ &+\mathrm{e}^{-\frac{\omega_D t}{2}}\left[\frac{1}{\sqrt{1-4\gamma/\omega_D}}\left(\frac{3}{\gamma\omega_D}-\frac{1}{\gamma^2}\right)\right.\\ &\times\sinh\left(\frac{\omega_D t}{2}\sqrt{1-\frac{4\gamma}{\omega_D}}\right)\end{aligned}$$

$$+\left(\frac{1}{\gamma\omega_D}-\frac{1}{\gamma^2}\right)\cosh\left(\frac{\omega_D t}{2}\sqrt{1-\frac{4\gamma}{\omega_D}}\right)\Bigg]\Bigg\}. \quad (4.10)$$

Equation (4.9) agrees with the result in ref. 26 which is obtained from a classical stochastic approach. By taking a limit $\omega_D \to \infty$ instead of taking $\hbar \to 0$, eq. (4.6) reproduces the result in the Ohmic case, eqs. (24) and (25) in ref. 18. Note that eqs. (4.6) and (4.7) reduce to the correlation function of a free rotator system by setting the bath coupling γ to zero.

5. Numerical Result

We now numerically demonstrate our results by taking a parameter from a rotational motion of methyl group ($-CH_3$) in a toluene molecule. We set $\mu = 2.062\,\mathrm{kg{\cdot}m^2}$ and introduce a parameter, $\alpha = \hbar/(2\mu) = 2.547 \times 10^{12}\,\mathrm{Hz}$ ($\hbar\alpha = 2.674 \times 10^{-22}\,\mathrm{J} = 1.666 \times 10^{-3}\,\mathrm{eV}$). We consider the case where the system is in a nonpolar solvent whose effects are commonly studied using the present model with the aid of the Langevin equation. By plotting the absorption spectra given by eqs. (2.5) and (4.6) for various cutoff frequencies of the bath mode ω_D, we study the effects of the colored noise.

Let us consider the case of the weakly damped rotator ($\gamma < \alpha$). Figure 1 shows the absorption spectra for the colored noise in (a) the quantum case [eq. (4.6)] and (b) the classical case [eq. (4.8)]. Each graph is depicted for different cutoff frequencies; $\omega_D = 0.17\gamma\,\mathrm{Hz}$ (solid line), $3.0\gamma\,\mathrm{Hz}$ (dashed line), and ∞, i.e., the Ohmic dissipation (dotted line), where $\gamma = 1.3 \times 10^{11}\,\mathrm{Hz}$ and $T = 1\,\mathrm{K}$.

Figure 1(a) is the spectral line shape for small ω_D (solid line). This line is well fitted by the Gaussian line except for near the zero frequency, where the peak rises at $\omega = \alpha$. As the cutoff frequency ω_D increases (the dashed and dotted lines), the peak becomes broader and shifts to the red. The increase of the line width with ω_D can be interpreted as the increase of effective damping strength $|\gamma(\omega)|$ with increasing ω_D, where $\gamma(\omega)$ is the damping kernel for the colored noise in Fourier space given by $\gamma(\omega) = \gamma/(1 - \mathrm{i}\omega/\omega_D)$. The red

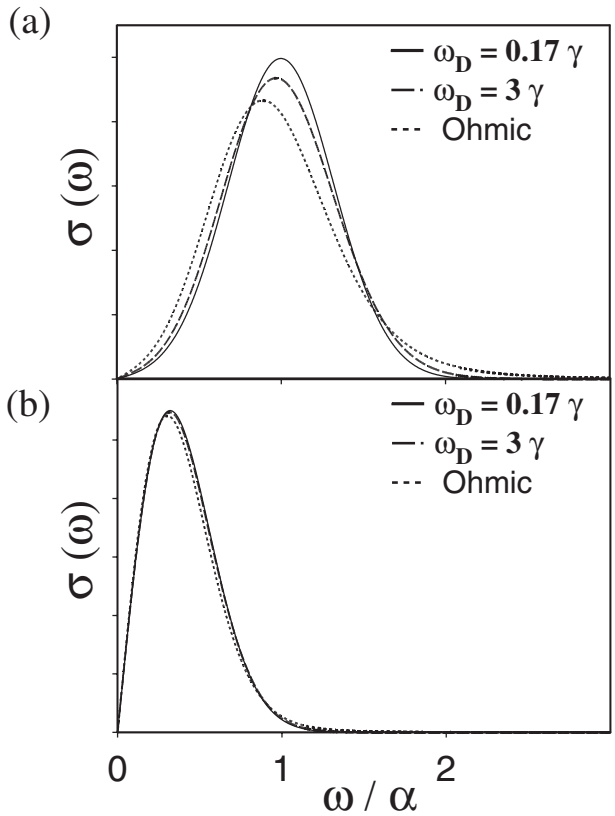

Fig. 1. (a) presents the absorption spectrum in the Gaussian–Markovian dissipation at the temperature $T = 1\,\mathrm{K}$ for the fixed damping strength $\gamma = 1.3 \times 10^{11}\,\mathrm{Hz}$ for different cutoff frequencies; $\omega_D = 0.17\gamma\,\mathrm{Hz}$ (solid line), $\omega_D = 3.0\gamma\,\mathrm{Hz}$ (dashed line), and $\omega_D = \infty$, i.e., the Ohmic dissipation case (dotted line). (b) shows the classical limit of (a).

shift of the peak with the increase in ω_D can be explained as follows. Since we consider the low temperature case, $T = 1\,\mathrm{K}$, the main contribution of the signal arises from the transition $|l = 0\rangle \to |l = 1\rangle$. From eqs. (2.5) and (4.6), the line shape for small ω_D (solid line) is expressed as

$$\sigma(\omega) = \frac{\sqrt{2\beta\mu\pi}}{4\hbar(1+\beta^2\hbar^2\gamma\omega_D/12)}\left(\mathrm{e}^{-\frac{\beta\mu}{2(1+\beta^2\hbar^2\gamma\omega_D)}(\omega-\alpha)^2} - \mathrm{e}^{-\frac{\beta\mu}{2(1+\beta^2\hbar^2\gamma\omega_D)}(\omega+\alpha)^2}\right). \quad (5.1)$$

The effective moment of inertia increases with the increase of ω_D, because the rotational motion is disturbed by the heat bath with the effective damping $|\gamma(\omega)|$. This is why the peak at $\omega = \hbar/(2\mu)$ is shifted to the red for large ω_D.

Figure 1(b) shows the absorption spectra for the classical case calculated from eq. (2.5) with eq. (4.6) by taking $\hbar \to 0$. To calculate each lines (solid, dashed, and dotted), we use the same parameters as Fig. 1(a). For small ω_D, eq. (5.1) is reduced to

$$\sigma(\omega) = \frac{\beta\omega}{4}\sqrt{2\beta\mu\pi}\,\mathrm{e}^{-\frac{\beta\mu}{2}\omega^2}. \quad (5.2)$$

Compared with the quantum case, the effects of ω_D are subtle. It can be understood in the following way. The spectral line shape is determined by the initial thermal distribution and dynamics of the system. In the quantum case, the kinetic energy of the system is discretized and, at low temperatures, the transition $|0\rangle \to |1\rangle$ strongly affects the line shape. In the classical case, however, a line shape profile is affected by the initial thermal distribution rather than the dynamics of the rotator; the kinetic energy and discrete states become continuous. Since ω_D, which changes the effective coupling strength $\gamma(\omega)$, plays a minor role in the initial thermal distribution, the line shapes do not depend so much on ω_D.

Next, we consider the effect of the noise correlation and the temperature for the strongly damped case, where γ satisfies $\gamma \gg \alpha$ and $\gamma \gg (\beta\hbar)^{-1}$ in which the damping effects are much larger than the quantum and thermal excitation effects. Figure 2 depicts the absorption spectra for different cutoff frequencies: $\omega_D/\gamma = 30$ (solid line), 0.2 (dashed line), and 0.1 (dotted line), for fixed

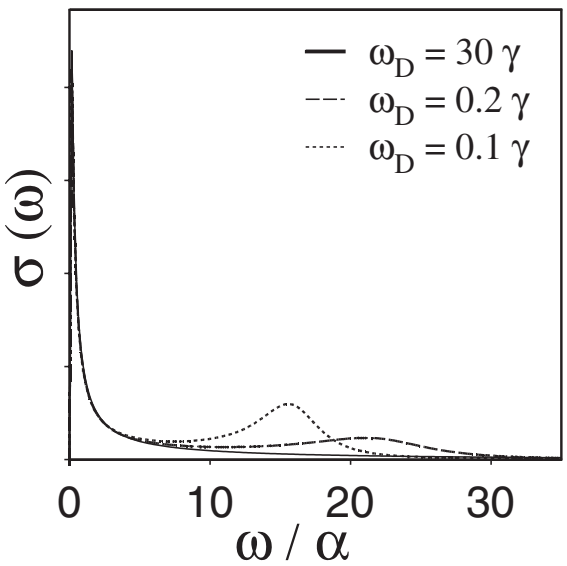

Fig. 2. The absorption spectra in a strongly damped rotator for different cutoff frequencies $\omega_D/\gamma = 30$ (solid line), 0.2 (dashed line), and 0.1 (dotted line) for fixed $\gamma = 1.3 \times 10^{14}$ Hz at $T = 50$ K.

$\gamma = 1.3 \times 10^{14}$ Hz at $T = 50$ K, while Fig. 3 describes the various cases of temperature: $T = 1$ (solid line), 50 (dashed line), and 100 K (dotted line) for fixed $\gamma = 1.3 \times 10^{14}$ Hz and $\omega_D = 0.1\gamma$ Hz. In Fig. 2, it was found that, with the increase of the noise correlation time $1/\omega_D$, the spectrum with one sharp peak near the zero frequency becomes bimodal. The new peak shifts to the red with decreasing ω_D. In Fig. 3, the spectral line shapes are the bimodal as shown in the dotted line of Fig. 2. In Fig. 3(a), as the temperature increases, the peak near the zero frequency shifts to the blue and becomes broader. In Fig. 3(b), the other peak at $\omega/\alpha \sim 15.8$ becomes broader with the increase in temperature. In order to understand such features, we employ the approximate expression of the two-time correlation function.

For large cutoff frequency satisfying $\omega_D > 4\gamma$ (solid line of Fig. 2), where $x_{1,2}$ defined by eq. (3.24) is the real number, the absorption spectra can be expressed as

$$\sigma(\omega) \simeq \frac{1}{2\mu\gamma}\left(\frac{\omega}{\omega^2 + (1/\beta\mu\gamma)^2} - \frac{\omega}{\omega^2 + (\Gamma_D + 1/\beta\mu\gamma)^2}\right), \tag{5.3}$$

where Γ_D is given by $\omega_D/2$ and γ for the cases $4\gamma/\omega_D \sim 1$ and $4\gamma/\omega_D \ll 1$, respectively, and $\Gamma_D = \gamma$ for the Gaussian-white limit ($\omega_D \to \infty$). Equation (5.3) reveals a sharp peak near $1/(\beta\mu\gamma)$ with the line width of about $1/(\beta\mu\gamma)$.

In eq. (5.3), the increase in γ plays the same role as the increase in the moment of inertia, which causes the decrease in the transition energy $\hbar\alpha(2l+1)$ corresponding to the transition $|l\rangle \to |l+1\rangle$. Hence the peak of the absorption spectrum shifts to the red with the increase in γ.

The spectral line width of the solid line in Fig. 2 becomes narrower as the damping constant γ becomes stronger. This behavior can be understood as follow. Due to the strong resistance of the heat bath, the rotator's motion halts quickly. In such a case, the time correlation function $(\mathrm{i}/\hbar)\langle[\cos\theta(t), \cos\theta(0)]\rangle$ is approximated by the constant $1/(2\mu\gamma)$. Therefore, the absorption spectra corresponding to the Fourier transformation of the time correlation function

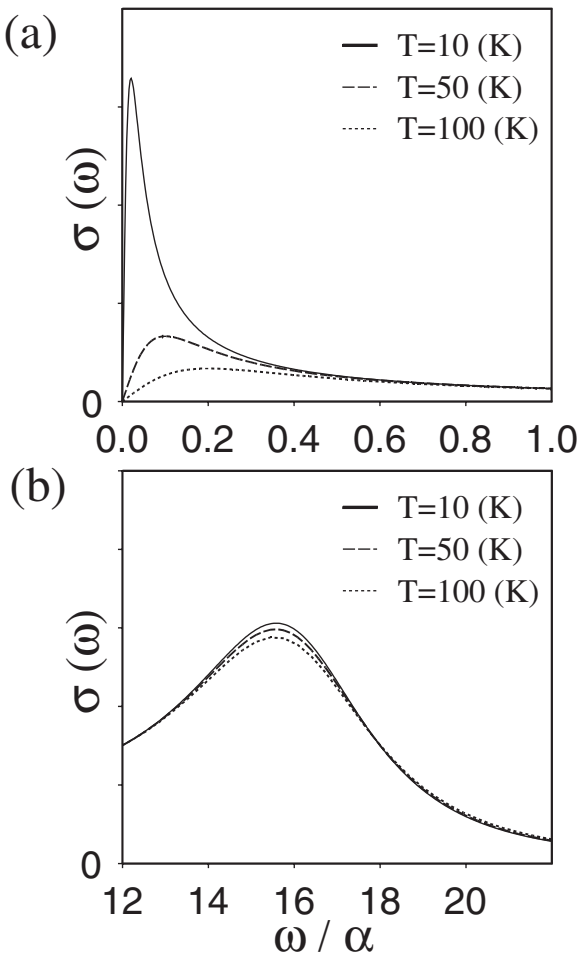

Fig. 3. (a) and (b) show the temperature dependence of absorption spectra in a strongly damped rotator around the peak close to zero frequency and the peak at $\omega/\alpha \sim 15.8$ indicated by the dotted line in Fig. 2. We present the results for different temperatures, $T = 10$ K (solid line), $T = 50$ K (dashed line), and $T = 100$ Hz (dotted line) for fixed $\gamma = 1.3 \times 10^{14}$ Hz and $\omega_D = 0.1\gamma$ Hz.

has the sharp peak for the strong damping.

For $\omega_D < 4\gamma$ (dashed and dotted lines of Fig. 2 and all lines of Fig. 3), we can see interesting features similar to the classical case,[26,27] which dose not appear in $\omega_D > 4\gamma$ case. In this case, $x_{1,2}$ is a complex number and the absorption spectra of the strongly damped oscillator is approximately described as

$$\sigma(\omega) = \sigma_1(\omega) + \sigma_2(\omega). \tag{5.4}$$

Here, $\sigma_1(\omega)$ and $\sigma_2(\omega)$ are defined by

$$\sigma_1(\omega) = \frac{\alpha}{\hbar\gamma}\frac{\omega}{\omega^2 + (2\alpha/\beta\hbar\gamma)^2}, \tag{5.5}$$

$$\sigma_2(\omega) = \frac{\alpha}{\hbar\gamma}\int_0^\infty \mathrm{d}t\mathrm{e}^{\mathrm{i}\omega t}R_2(t), \tag{5.6}$$

where

$$R_2(t) \equiv \frac{(2\gamma/\omega_D)}{\sqrt{(4\gamma/\omega_D) - 1}}\mathrm{e}^{-\left(\frac{\omega_D}{2} + \frac{2\alpha}{\beta\hbar\gamma}\right)t} \times \sin\left(\frac{\omega_D t}{2}\sqrt{\frac{4\gamma}{\omega_D} - 1} - \phi_x\right). \tag{5.7}$$

In eq. (5.7), the phase ϕ_x is given by

$$\cos\phi_x = \frac{\omega_D}{2\gamma}\left(\frac{2\gamma}{\omega_D} - 1\right), \tag{5.8}$$

$$\sin\phi_x = \frac{\omega_D}{2\gamma}\sqrt{\frac{4\gamma}{\omega_D} - 1}. \tag{5.9}$$

The first term $\sigma_1(\omega)$ leads to the peak close to the zero frequency in the absorption spectrum, whose position, line width, and intensity are given by about $2\alpha/(\beta\hbar\gamma)$, $2\alpha/(\beta\hbar\gamma)$, and $\gamma\beta\hbar/\alpha$, respectively. We shall call it the low-frequency peak. The second term $\sigma_2(\omega)$ causes the other peak at high frequency ($\omega/\alpha \simeq 16$ in the dotted line of Fig. 2 and in all lines of Fig. 3 and $\omega/\alpha \simeq 23$ in the dashed line of Fig. 2) that shall be called the high-frequency peak. We note that $R_2(t)$ in eq. (5.7) is the same form as the correlation function of the harmonic oscillator system in the Ohmic dissipation whose frequency and damping are given by $\sqrt{\gamma\omega_D}$ and ω_D besides the factor $\mathrm{e}^{-2\alpha t/(\beta\hbar\gamma)}$.[10,12] The position of the low-frequency peak is then given by $(\omega_D/2)\sqrt{(4\gamma/\omega_D) - 1}$. Equations (5.6) and (5.7) imply that the high-frequency peak has a blue shift and becomes broader for large ω_D.

As will shown below, the high-frequency and low-frequency peaks can be interpreted to originate from the librational and strongly damped free rotational motions, respectively. In the slow modulation case, the bath oscillators localize near zero mode due to the small cutoff frequency. For large γ, the motion of the system decays much faster than the characteristic time scale of the bath oscillation, so that the system cannot recover the rotational symmetry given in the Langevin equation (2.2). Such a feature can be shown with the aid of the Langevin equation. For small ω_D, by integrating by part the second term in the L.H.S. of the Langevin equation (2.2) and neglecting the term proportional to ω_D^2, we describe the equation of motion as

$$\mu\ddot{\theta}(t) + \mu\gamma\omega_D\theta(t) - \mu\gamma\omega_D \mathrm{e}^{\omega_0(t-t_l)\theta(t_l)} = R(t). \tag{5.10}$$

From eq. (5.10), the counter term in the Hamiltonian (2.1), $(\mu\gamma\omega_D/2)\theta^2$, is regarded as the additional potential in the second term of eq. (5.10), which leads the system librational motion with the frequency $\sqrt{\gamma\omega_D}$ corresponding to the high-frequency peak. With the increase in ω_D, the effective damping $|\gamma(\omega)|$ becomes strong, and then the system librational motion decays faster. Hence, the width of the high-frequency peak becomes broader with increasing ω_D. The low-frequency peak corresponds to the free rotational motion recovering the rotational symmetry of the total Hamiltonian (2.1). We note that the high-frequency peak cannot be seen for the fast modulation case where the cutoff frequency satisfies $\omega_D > 4\gamma$, including the case of the Gaussian-white noise, because, if the bath oscillational motion is faster than the decay of the motion of the system, the system maintains the rotational symmetry and the librational motion does not happen. The high-frequency peak can also be observed in Brownian oscillator system in the slow modulation case, even if the oscillator frequency of the system is zero.[28] In the Brownian oscillator system, the high-frequency peak arises from the vibrational motion caused by the broken translational symmetry. Such a vibrational motion and the translational symmetry correspond to the librational motion and the rotational symmetry in the rotator system.

As can be seen in Fig. 3(a), the low-frequency peak corresponding to the strongly damped rotational motion shifts to the blue and becomes broader with the increase in the temperature. From the same argument in the case $\omega_D > 4\gamma$, the behavior of this peak implies the decrease of the effective damping strength of the strongly damped rotational motion, which arises from the suppression of the system-bath coupling by the thermal fluctuation. In Fig. 3(b), the high-frequency peak corresponding to the librational motion observed in the slow modulation case becomes broader with the increase in the temperature. This can be explained as follows. Since the thermal fluctuation decreases the time scale of the bath oscillation with the increase in the temperature, the system easily recovers the rotation symmetry and the librational motion caused by the rotational symmetry breaking decays fast.

6. Conclusion

In this paper, we investigate the effect of the colored noise in the rotational Brownian motion with the assumption that the Gaussian–Markovian random torque acts on the dipole moment. We calculate the two-time correlation function in the Gaussian–Markovian dissipation with the aid of a generating functional obtained in the previous letter. Using the parameter employed from the rotational motion of a methyl group, we plot the absorption spectra related to the two-time correlation function for the different temperatures, damping strength, and cutoff frequencies of the spectral distribution function.

For the weakly damped case at the low temperature, the spectral line shape is determined by the system dynamics in which the discritization of the kinetic energy of the system is reflected. The peak rises at $\hbar/(2\mu)$ corresponding to the transition $|0\rangle \to |1\rangle$. Since the cutoff frequency of the spectral distribution function, ω_D, plays a role in increasing the effective moment of inertia, the peak position shifts to the red with the increase in ω_D.

For the strongly damped case, we see the bimodal line shape for small ω_D, i.e., the slow modulation case. One of the peaks rises near the zero frequency, which corresponds to the overdamped motion of the rotator. The other peak is found at $\omega \simeq \sqrt{\gamma\omega_D}$, which corresponds to the librational motion caused by the coupling to the bath oscillators that localize near the zero mode because of the small cutoff frequency of the spectral distribution function. By increasing ω_D, we find that the spectral line has a peak near the zero frequency in the fast modulation case. Hence, the peak corresponding to the librational motion is not found in the Gaussian-white noise.

In the present study, we restricted our study to the linear-linear coupling between the system and the bath and obtained the continuous spectra. However, in the many realistic problems, the absorption spectra show discrete lines. To take into account experiments, it is necessary to consider another system-bath coupling, *e.g.*, $-\sum_i q_i \cos n\theta$ where n is decided by the properties of the environment. Such problems are left for future studies.

Acknowledgements

We wish to thank Du Side for useful discussions. We thank financial support of a Grant-in-Aid for Scientific Research (B) (12440171) from Japan Society for the Promotion of Science.

Appendix A: Derivation of the Classical Langevin Equation

In this Appendix, we derive the classical Langevin equation from the Hamiltonian (2.1). The canonical equations of motion for classical trajectory are

$$\dot{\theta}(t) = \frac{1}{\mu} L(t), \tag{A·1}$$

$$\dot{L}(t) = -\sum_i c_i \left(q_i(t) - \frac{c_i \theta(t)}{m_i \omega_i^2} \right), \tag{A·2}$$

$$\dot{q}_i(t) = \frac{1}{m_i} p_i(t), \tag{A·3}$$

$$\dot{p}_i = -m_i \omega_i^2 q_i(t) + c_i \theta(t). \tag{A·4}$$

Here, q_i and p_i represent the coordinate and momentum of the ith bath oscillator mapped on the classical trajectory. From eqs. (A·1), (A·2), (A·3) and (A·4), the variables $\theta(t)$ and $q_i(t)$ satisfy the equation

$$\mu \ddot{\theta}(t) = -\sum_i c_i \left(q_i(t) - \frac{c_i \theta(t)}{m_i \omega_i^2} \right), \tag{A·5}$$

$$m_i \ddot{q}_i(t) = -m_i \omega_i^2 q_i(t) + c_i \theta(t). \tag{A·6}$$

Equation (A·6) can be solved explicitly, i.e.,

$$q_i(t) = q_i(t_I) \cos[\omega_i(t - t_I)] + \frac{p_i(t_I)}{m_i \omega_i} \sin[\omega_i(t - t_I)] + \int_{t_I}^{t} \mathrm{d}t' \sin[\omega_i(t - t')] \frac{c_i \theta(t')}{m_i \omega_i}. \tag{A·7}$$

Substitution of (A·7) into (A·5) and the use of the relation

$$\begin{aligned} &\int_{t_I}^{t} \mathrm{d}t' \sin[\omega_i(t - t')] \frac{c_i \theta(t')}{m_i \omega_i} \\ &= \frac{c_i \theta(t)}{m_i \omega_i^2} - \cos[\omega_i(t - t_I)] \frac{c_i \theta(t_I)}{m_i \omega_i^2} - \int_{t_I}^{t} \mathrm{d}t' \cos[\omega_i(t - t')] \frac{c_i \dot{\theta}(t)}{m_i \omega_i^2} \end{aligned} \tag{A·8}$$

yield

$$\begin{aligned} &\mu \ddot{\theta}(t) + \sum_i c_i \int_{t_I}^{t} \mathrm{d}t' \cos[\omega_i(t - t')] \frac{c_i \dot{\theta}(t')}{m_i \omega_i^2} \\ &= -\sum_i c_i \left[\sin[\omega_i(t - t_I)] \frac{p_i(t_I)}{m_i \omega_i} + \cos[\omega_i(t - t_I)] \left(q_i(t_I) - \frac{c_i \theta(t_I)}{m_i \omega_i^2} \right) \right]. \end{aligned} \tag{A·9}$$

Using the definitions

$$\eta(t - t') = \sum_i \cos[\omega_i(t - t')] \frac{c_i^2}{m_i \omega_i^2}, \tag{A·10}$$

$$R(t) = -\sum_i c_i \left[\sin[\omega_i(t - t_I)] \frac{p_i(t_I)}{m_i \omega_i} + \cos[\omega_i(t - t_I)] \left(q_i(t_I) - \frac{c_i \theta(t_I)}{m_i \omega_i^2} \right) \right], \tag{A·11}$$

we obtain the Langevin equation (2.2). For the thermal equilibrium initial state with the inverse temperature $\beta = 1/(k_B T)$ at $t = t_I$, the expectation value is given by

$$\langle X \rangle_I \equiv \frac{\int_{-\infty}^{\infty} \left[\prod_i \frac{\mathrm{d}p_i}{2\pi\hbar} \right] \int_{-\infty}^{\infty} \left[\prod_i \mathrm{d}q_i \right] \int_{-\infty}^{\infty} \frac{\mathrm{d}L}{2\pi\hbar} \int_{-\pi}^{\pi} \mathrm{d}\theta \mathrm{e}^{-\beta H(\theta(t_I), L(t_I), q_i(t_I), p_i(t_I))} X}{\int_{-\infty}^{\infty} \left[\prod_i \frac{\mathrm{d}p_i}{2\pi\hbar} \right] \int_{-\infty}^{\infty} \left[\prod_i \mathrm{d}q_i \right] \int_{-\infty}^{\infty} \frac{\mathrm{d}L}{2\pi\hbar} \int_{-\pi}^{\pi} \mathrm{d}\theta \mathrm{e}^{-\beta H(\theta(t_I), L(t_I), q_i(t_I), p_i(t_I))}}. \tag{A·12}$$

Hence the fluctuation force $R(t)$ satisfies the relations (2.3) and (2.4).

Appendix B: Factorization of the Generating Functional

In this Appendix, we represent the generating functional as the product of the rotator part and the bath coordinate part. We set the Hamiltonian including the source term as

$$\hat{H}_{\mathcal{K}} \equiv \hat{H} - \sum_{n=-\infty}^{\infty} \mathcal{K}^{(n)}(t) \mathrm{e}^{\mathrm{i}n\theta} \tag{B·1}$$

As shown in eq. (3.2), the correlation function of $\cos\theta$ is then expressed by setting $\mathcal{K}^{(n)}(t) = \mathcal{K}(t)/2$ for $n = \pm 1$ and $\mathcal{K}^{(n)}(t) = 0$ for the others. By rewriting the new coordinate

$\hat{y}_i$ and $\hat{p}_{yi}$ as in §3 and performing the unitary transformation $\hat{X}_1 \equiv \exp[-(\mathrm{i}/\hbar)\theta \sum_i \hat{p}_{yi}]$, the Hamiltonian becomes

$$\hat{H}^{(1)}_{\mathcal{K}} \equiv \hat{X}_1^\dagger \hat{H}_{\mathcal{K}} \hat{X}_1 = \frac{1}{2\mu}\left(L - \sum_i \hat{p}_{yi}\right)^2 + \sum_i \left(\frac{\hat{p}_{yi}^2}{2\mu_i} + \frac{\mu_i \omega_i^2}{2}\hat{y}_i^2\right) - \sum_{n=-\infty}^{\infty} \mathcal{K}^{(n)}(t)\mathrm{e}^{\mathrm{i}n\theta}, \quad (\mathrm{B}\cdot 2)$$

where we have used $\hat{X}_1^\dagger L \hat{X}_1 = L - \sum_i \hat{p}_{yi}$ and $\hat{X}_1^\dagger \hat{y}_i \hat{X}_1 = \hat{y}_i + \theta$. Since the Hamiltonian $\hat{H}^{(1)}_{\mathcal{K}}$ satisfies the periodic boundary condition, we use the eigenstates of the angular momentum, $S_l(\theta) = \mathrm{e}^{\mathrm{i}l\theta}/\sqrt{2\pi}$, defined by $LS_l(\theta) = \hbar l S_l(\theta)$ and formally express the completeness relation $\sum_{l=-\infty}^{\infty} S_l^{(1)*}(\theta) S_l^{(1)}(\theta') = \delta(\theta - \theta')$, as

$$S_l^{(1)}(\theta) = \langle \theta | l \rangle, \quad \sum_{l=-\infty}^{\infty} |l\rangle\langle l| = 1, \qquad \langle \theta | \theta' \rangle = \delta(\theta - \theta'), \quad \int_{-\pi}^{\pi} \mathrm{d}\theta |\theta\rangle\langle\theta| = 1. \quad (\mathrm{B}\cdot 3)$$

Using $H^{(1)}_{\mathcal{K}}$, the generating functional, eq. (3.1), is rewritten as

$$Z[\mathcal{K}] = \mathrm{Tr}\left\{\hat{\rho}_I^{(1)\mathcal{K}_3} \hat{U}^{(1)\dagger}_{\mathcal{K}_2}(\infty, t_I) \hat{U}^{(1)}_{\mathcal{K}_1}(\infty, t_I)\right\}, \quad (\mathrm{B}\cdot 4)$$

where $\hat{\rho}_I^{(1)\mathcal{K}}$ and $\hat{U}^{(1)}_{\mathcal{K}}(\infty, t_I)$ are defined by $\hat{\rho}_I^{(1)\mathcal{K}} \equiv \mathrm{T}_\tau \exp[-(1/\hbar)\int_0^{\beta\hbar} \mathrm{d}\tau \hat{H}^{(1)}_{\mathcal{K}}]$ and $\hat{U}^{(1)}_{\mathcal{K}}(\infty, t_I) \equiv \mathrm{T}_t \exp[-(\mathrm{i}/\hbar)\int_{t_I}^{\infty} \mathrm{d}t \hat{H}^{(1)}_{\mathcal{K}}]$. By expanding $Z[\mathcal{K}]$ by the source term $V_{\mathcal{K}} \equiv -\sum_{n=-\infty}^{\infty} \mathcal{K}^{(n)}(t)\mathrm{e}^{\mathrm{i}n\theta}$ and inserting the relations $1 = \sum_l |l\rangle\langle l| = \hat{X}_2 \sum_l |l\rangle\langle l| \hat{X}_2^\dagger$ where $\hat{X}_2 = \exp[(\mathrm{i}/\hbar)\sum_i r_i L \hat{y}_i]$, $Z[\mathcal{K}]$ is written as

$$\begin{aligned} Z[\mathcal{K}] &= \sum_{N=0}^{\infty} \frac{1}{N!} \int_C \mathrm{d}t_1 \mathrm{d}t_2 \ldots \mathrm{d}t_N \left(-\frac{\mathrm{i}}{\hbar}\right)^N \mathrm{Tr}\left[\mathrm{e}^{-\beta \hat{H}^{(1)}} \left(\mathrm{T}_C V_{\mathcal{K}}(\theta(t_1)) V_{\mathcal{K}}(\theta(t_2)) \ldots V_{\mathcal{K}}(\theta(t_N))\right)\right] \\ &= \sum_{N=0}^{\infty} \frac{1}{N!} \int_C \mathrm{d}t_1 \mathrm{d}t_2 \ldots \mathrm{d}t_N \left(-\frac{\mathrm{i}}{\hbar}\right)^N \mathrm{Tr}_B \sum_{l=-\infty}^{\infty} \sum_{l_1,\ldots,l_N} \sum_{l'_1,\ldots,l'_N} \\ &\quad \times \left(\prod_{k=2}^{N+1} \langle l_k | \mathrm{e}^{-\mathrm{i}l_k \sum_i r_i \hat{y}_i} \mathrm{e}^{-\frac{\mathrm{i}}{\hbar}\hat{H}^{(1)}(t_k - t_{k-1})} \mathrm{e}^{\mathrm{i}l'_{k-1} \sum_i r_i \hat{y}_i} | l'_{k-1} \rangle \right. \\ &\quad \times \left. \langle l'_{k-1} | \mathrm{e}^{-\mathrm{i}l'_{k-1} \sum_i r_i \hat{y}_i} V_{\mathcal{K}}(\theta_{k-1}) \mathrm{e}^{\mathrm{i}l_{k-1} \sum_i r_i \hat{y}_i} | l_{k-1} \rangle \right) \\ &\quad \times \left. \langle l_1 | \mathrm{e}^{-\mathrm{i}l_1 \sum_i r_i \hat{y}_i} \mathrm{e}^{-\frac{\mathrm{i}}{\hbar}\hat{H}^{(1)}(t_1 - t_0)} \mathrm{e}^{\mathrm{i}l_0 \sum_i r_i \hat{y}_i} | l_0 \rangle \right|_{l_{N+1} = l_0 = l}, \end{aligned} \quad (\mathrm{B}\cdot 5)$$

where $\theta_i \equiv \theta(t_i)$, $\hat{H}^{(1)} = \hat{X}_1^\dagger \hat{H} \hat{X}_1$, and Tr_B implies the trace over the bath coordinate, $\hat{p}_{yi}$ and $\hat{y}_i$. The periodic boundary condition $l_0 = l_{N+1}$ arises from the trace over the system coordinate. Since the matrix elements $\langle l|A|l'\rangle$ is calculated by $\langle l|A|l'\rangle = \int_{-\pi}^{\pi} \mathrm{d}\theta [\mathrm{e}^{-\mathrm{i}(l-l')\theta}/(2\pi)]A$, we have

$$\langle l_k | \mathrm{e}^{-\mathrm{i}l_k \sum_i r_i \hat{y}_i} \mathrm{e}^{-\frac{\mathrm{i}}{\hbar}\hat{H}^{(1)}(t_k - t_{k-1})} \mathrm{e}^{\mathrm{i}l'_k \sum_i r_i \hat{y}_i} | l'_k \rangle = \mathrm{e}^{-\frac{\mathrm{i}}{\hbar}\hat{\tilde{H}}_{l_k}(t_k - t_{k-1})} \delta_{l_k, l'_k}, \quad (\mathrm{B}\cdot 6)$$

$$\langle l'_k | \mathrm{e}^{-\mathrm{i}l'_k \sum_i r_i \hat{y}_i} V_{\mathcal{K}}(\theta_k) \mathrm{e}^{\mathrm{i}l_k \sum_i r_i \hat{y}_i} | l_{k-1} \rangle = -\sum_{n_k=-\infty}^{\infty} \mathcal{K}^{(n_k)}(t_k) \mathrm{e}^{-\mathrm{i}n_k \sum_i r_i \hat{y}_i} \delta_{l'_k, l_k + n_k}, \quad (\mathrm{B}\cdot 7)$$

where $\hat{\tilde{H}}_l \equiv \hat{\tilde{H}}|_{L=\hbar l}$ in which $\hat{\tilde{H}}$ is given by eq. (3.6). By substituting eqs. (B·6) and (B·7) into eq. (B·5) and summing up over $l'_1, l'_2, \ldots, l'_N$, $Z[\mathcal{K}]$ is rewritten as

$$Z[\mathcal{K}] = \sum_{N=0}^{\infty} \frac{1}{N!} \int_C \mathrm{d}t_1 \mathrm{d}t_2 \ldots \mathrm{d}t_N \left(\frac{\mathrm{i}}{\hbar}\right)^N \times \sum_{n_1,\ldots,n_N} \mathcal{K}^{(n_1)}(t_1) \ldots \mathcal{K}^{(n_N)}(t_N) \left(Z_S^{(n_1,\ldots,n_N)} Z_B^{(n_1,\ldots,n_N)}\right) \quad (\mathrm{B}\cdot 8)$$

where $Z_S^{(n_1,\ldots,n_N)}$ and $Z_B^{(n_1,\ldots,n_N)}$ are given by

$$Z_S^{(n_1,\ldots,n_N)} = \sum_{l=-\infty}^{\infty} \sum_{l_1,\ldots,l_N} \left(\prod_{k=1}^{N+1} \mathrm{e}^{-\frac{\mathrm{i}}{\hbar}\tilde{H}_S(L=\hbar l_k)(t_k - t_{k-1})}\right) \times \delta_{l_{N+1}, l_N + n_N} \delta_{l_N, l_{N-1} + n_{N-1}} \ldots \delta_{l_2, l_1 + n_1} \Bigg|_{l_{N+1} = l_0 = l} \quad (\mathrm{B}\cdot 9)$$

$$Z_B^{(n_1,\ldots,n_N)} = \mathrm{Tr}_B \left(\prod_{k=2}^{N+1} \mathrm{e}^{-\frac{\mathrm{i}}{\hbar}\tilde{H}_B(t_k - t_{k-1})} \mathrm{e}^{-\mathrm{i}n_{k-1} \sum_i r_i \hat{y}_i}\right) \mathrm{e}^{-\frac{\mathrm{i}}{\hbar}\tilde{H}_B(t_1 - t_0)}, \quad (\mathrm{B}\cdot 10)$$

in which $\tilde{H}_S$ and $\tilde{H}_B$ are given by eqs. (3.7) and (3.8), respectively. By means of $Z_S[J]$ and $Z_B[J]$ defined by eqs.

(3.10) and (3.11), eqs. (B·9) and (B·10) are expressed as

$$Z_S^{(n_1,\dots,n_N)} = (Z_S[J])_{J(s)/\hbar=\sum_{i=1}^N n_i\delta(s-t_i)}, \tag{B·11}$$

$$Z_B^{(n_1,\dots,n_N)} = (Z_B[J])_{J(s)/\hbar=\sum_{i=1}^N n_i\delta(s-t_i)}. \tag{B·12}$$

Therefore we find

$$\begin{aligned}\mathrm{Tr}(\mathrm{T}_C \mathrm{e}^{\mathrm{i}n_1\theta(t_1)}\dots \mathrm{e}^{\mathrm{i}n_N\theta(t_N)}) &= \left(\frac{\hbar}{\mathrm{i}}\right)^N \frac{\delta^N Z[\mathcal{K}]}{\delta_C\mathcal{K}^{(n_1)}(t_1)\dots\delta_C\mathcal{K}^{(n_N)}(t_N)} \\ &= (Z_S[J]Z_B[J])_{J(s)/\hbar=\sum_{i=1}^N n_i\delta_C(s-t_i)},\end{aligned} \tag{B·13}$$

which gives eq. (2.5).

Appendix C: The Generating Functional from the Bath Degrees of the Freedom

To calculate the bath part of the generating functional $Z_B[J]$, we introduce the sets of eigenstates $|\boldsymbol{y}\rangle$ and $|\boldsymbol{p}\rangle$ defined by $\hat{y}_i|\boldsymbol{y}\rangle = y^{(i)}|\boldsymbol{y}\rangle$ and $\hat{p}_{yi}|\boldsymbol{p}\rangle = p_y^{(i)}|\boldsymbol{y}\rangle$, respectively. The completeness relations are given by

$$\int_{-\infty}^{\infty}\left[\prod_i \mathrm{d}y^{(i)}\right]|\boldsymbol{y}\rangle\langle\boldsymbol{y}| = 1, \quad \int_{-\infty}^{\infty}\left[\prod_i \frac{\mathrm{d}p_y^{(i)}}{2\pi\hbar}\right]|\boldsymbol{p}_y\rangle\langle\boldsymbol{p}_y| = 1. \tag{C·1}$$

Their overlaps are expressed as $\langle\boldsymbol{y}|\boldsymbol{p}_y\rangle = \mathrm{e}^{\frac{\mathrm{i}}{\hbar}\boldsymbol{p}_y\cdot\boldsymbol{y}}$, $\langle\boldsymbol{y}|\boldsymbol{y}'\rangle = \delta(\boldsymbol{y}-\boldsymbol{y}')$, and $\langle\boldsymbol{p}_y|\boldsymbol{p}_y'\rangle = \delta(\boldsymbol{p}_y-\boldsymbol{p}_y')$. Dividing the time interval on the contour time path into $N+1$ pieces $(t_0 = t_I, t_1, \dots, t_N, t_{N+1} = t_I - \mathrm{i}\beta\hbar)$ and inserting the completeness relation eq. (C·1), we have

$$\begin{aligned}Z_B[J] = \lim_{N\to\infty}&\int\left[\prod_i \mathrm{d}y_0^{(i)}\right]\int\left[\prod_i\prod_{k=1}^N \mathrm{d}y_k^{(i)}\right]\int\left[\prod_i\prod_{k=0}^N \frac{\mathrm{d}p_{yk}^{(i)}}{2\pi\hbar}\right] \\ &\times\exp\left[\frac{\mathrm{i}}{\hbar}\sum_{k=0}^N\left\{\sum_i p_{yk}^{(i)}(y_{k+1}^{(i)}-y_k^{(i)})\right.\right. \\ &-\epsilon_k\left[\sum_i\left(\frac{(p_{yk}^{(i)})^2}{2\mu_i}+\frac{1}{2}\mu_i\omega_i^2(y_k^{(i)})^2+J(t_k)r_iy_k^{(i)}\right)\right. \\ &\left.\left.\left.+\frac{1}{2\mu}\left(\sum_i p_{yk}^{(i)}\right)^2\right]\right\}\right]\Bigg|_{\boldsymbol{y}_{N+1}=\boldsymbol{y}_0},\end{aligned} \tag{C·2}$$

where $\epsilon_i = t_{i+1} - t_i$ $(i = 1, 2, \dots, N)$. The periodic boundary condition $\boldsymbol{y}_{N+1} = \boldsymbol{y}_0$ arises from the "trace" operation involved in the definition of the generating functional. Since the variables $p_{yk}^{(i)}$ are integrated out in each k, the bath part of the generating functional $Z_B[J]$ becomes

$$\begin{aligned}Z_B[J] = \lim_{N\to\infty}&\int\left[\prod_i \mathrm{d}y_0^{(i)}\right]\int\left[\prod_i\prod_{k=1}^N \mathrm{d}y_k^{(i)}\right] \\ &\times\left[\prod_{k=0}^N\left\{\prod_i\left(\frac{\pi\hbar}{\mathrm{i}\epsilon}\right)^{\frac{1}{2}}\frac{1}{2\pi\hbar}\right\}\sqrt{\frac{1}{\det A}}\right] \\ &\times\exp\left[\frac{\mathrm{i}}{\hbar}\sum_{k=0}^N\left\{\frac{1}{4\epsilon_k}(\boldsymbol{y}_{k+1}-\boldsymbol{y}_k)^T A^{-1}(\boldsymbol{y}_{k+1}-\boldsymbol{y}_k)\right.\right. \\ &\left.\left.\left.-\epsilon_k\sum_i\left(\frac{1}{2}\mu_i\omega_i^2(y_k^{(i)})^2+J(t_k)r_iy_k^{(i)}\right)\right\}\right]\Bigg|_{\boldsymbol{y}_{N+1}=\boldsymbol{y}_0},\end{aligned} \tag{C·3}$$

where the matrix A is defined as $A_{i,j} = (1/2\mu_i)\delta_{i,j} + (1/2\mu)$. The determinant of A is given by

$$\det A = \left(\prod_i \frac{1}{2\mu_i}\right)\left(1+\frac{\sum_i\mu_i}{\mu}\right). \tag{C·4}$$

With the use of the relations

$$\left(A_1^{-1}A_2\right)^l = \left(\frac{\sum_i\mu_i}{\mu}\right)^{l-1}\left(A_1^{-1}A_2\right), \tag{C·5}$$

and $(A_1^{-1}A_2A_1^{-1})_{i,j} = (2/\mu)\mu_i\mu_j$, where $(A_1)_{i,j} \equiv (1/2\mu_i)\delta_{i,j}$ and $(A_2)_{i,j} \equiv 1/2\mu$, the matrix A^{-1} is rewritten as

$$A^{-1} = A_1^{-1} - \frac{2\mu_i\mu_j}{\mu'}. \tag{C·6}$$

From (C·6),

$$\boldsymbol{x}^T A^{-1}\boldsymbol{x} = \sum_i 2\mu_i x_i^2 - \frac{2}{\mu'}\left(\sum_i \mu_i x_i\right)^2. \tag{C·7}$$

Substituting eqs. (C·4) and (C·7) into eq. (C·3), we obtain

$$Z_B[J] = \int_C [\mathrm{d}\boldsymbol{y}]\mathrm{e}^{\frac{\mathrm{i}}{\hbar}\tilde{S}_B{}^J}, \tag{C·8}$$

where $\tilde{S}_B{}^J$ is the action given by

$$\begin{aligned}\tilde{S}_B{}^J = \frac{1}{2}\sum_{i,j}\int_C \mathrm{d}t\, y^{(i)}(t)\Bigg(&-\delta_{i,j}\mu_i\frac{\mathrm{d}^2}{\mathrm{d}t^2} \\ &+\frac{1}{\mu'}\mu_i\mu_j\frac{\mathrm{d}^2}{\mathrm{d}t^2}-\mu_i\omega_i^2\delta_{i,j}\Bigg)y^{(j)}(t) \\ &-\sum_i\int_C \mathrm{d}tJ(t)r_iy^{(i)}(t).\end{aligned} \tag{C·9}$$

Since the action $\tilde{S}_B{}^J$ is bilinear in $\boldsymbol{y}$, we can integrate over $\boldsymbol{y}$ and obtain

$$\begin{aligned}Z_B[J] &= \int_C [\mathrm{d}\boldsymbol{y}]\mathrm{e}^{\frac{\mathrm{i}}{\hbar}\left(-\int_C \mathrm{d}t\mathrm{d}t'\,\boldsymbol{y}(t)K^{-1}(t,t')\boldsymbol{y}(t')+\int_C \mathrm{d}t\,\boldsymbol{J}(t)\cdot\boldsymbol{y}\right)} \\ &= \mathrm{e}^{\frac{\mathrm{i}}{2\hbar}\int_C \mathrm{d}t\mathrm{d}t'\,\boldsymbol{J}(t)K(t,t')\boldsymbol{J}(t')}Z_B[J=0],\end{aligned} \tag{C·10}$$

where

$$\begin{aligned}\left(K^{-1}\right)_{i,j}(t,t') = \Bigg[&\delta_{i,j}\mu_i\frac{\mathrm{d}^2}{\mathrm{d}t^2}-\frac{1}{\mu+\sum_i\mu_i}\mu_i\mu_j\frac{\mathrm{d}^2}{\mathrm{d}t^2} \\ &+\mu_i\omega_i^2\delta_{i,j}\Bigg]\delta_C(t-t'),\end{aligned} \tag{C·11}$$

$$J_i(t) = -J(t_k)r_i. \tag{C·12}$$

By introducing the notation $J_+ = (J_1+J_2)/2$ and $J_- = J_1 - J_2$ and using eq. (C·12), the exponent in eq. (C·10) is expressed as

$$\int_C \mathrm{d}t\mathrm{d}t' \boldsymbol{J}(t)K(t,t')\boldsymbol{J}(t')$$
$$= \int_{t_I}^{\infty}\mathrm{d}t\int_{t_I}^{\infty}\mathrm{d}t'\sum_{i,j} r_i\Big(2J_-(t)K_{i,j}^{(+-)}(t-t')J_+(t')$$
$$+ J_-(t)K_{i,j}^{(++)}(t-t')J_-(t')\Big)r_j$$
$$- 2\mathrm{i}\int_{t_I}^{\infty}\mathrm{d}t\int_0^{\beta\hbar}\mathrm{d}\tau\sum_{i,j} r_iJ_-(t)K_{i,j}^{(+3)}(t,\tau)J_3(\tau)r_j$$
$$- \int_0^{\beta\hbar}\mathrm{d}\tau\int_0^{\beta\hbar}\mathrm{d}\tau'\sum_{i,j} r_iJ_3(\tau)K_{i,j}^{(33)}(\tau-\tau')J_3(\tau')r_j, \tag{C·13}$$

where $K_{i,j}^{(+-)} = K_{i,j}^{11} - K_{i,j}^{12}$, $K_{i,j}^{(++)} = (K_{i,j}^{11} + K_{i,j}^{12})/2$, $K_{i,j}^{(+3)} = K_{i,j}^{13} = K_{i,j}^{23}$, and $K_{i,j}^{(33)} = K_{i,j}^{33}$, in which $K_{i,j}^{\alpha_1\alpha_2}(t,t')$ implies $t \in C_{\alpha_1}$ and $t' \in C_{\alpha_2}$. Here, $K_{i,j}(t,t')$ is the propagator defined by $K_{i,j}(t,t') = (\mathrm{i}/\hbar)[\mathrm{Tr}\,\mathrm{e}^{-\beta\tilde{H}_B}(\mathrm{T}_C\hat{y}_i^{(B)}(t)\hat{y}_i^{(B)}(t'))]/\mathrm{Tr}\,\mathrm{e}^{-\beta\tilde{H}_B}$ where $\hat{y}_i^{(B)}(t) = \mathrm{e}^{\mathrm{i}\tilde{H}_Bt/\hbar}\hat{y}_i^{(B)}\mathrm{e}^{-\mathrm{i}\tilde{H}_Bt/\hbar}$, which satisfies the relation in the Fourier-Laplace representation:

$$K_{i,j}^{(+3)}(z,\nu_n) = \frac{\mathrm{i}}{z+\nu_n}\Big(K_{i,j}^{(+-)}(\nu_n) - K_{i,j}^{(+-)}(z)\Big), \tag{C·14}$$
$$K_{i,j}^{(++)}(z) = \frac{1}{2}\sum_{n=-\infty}^{\infty}\mathrm{e}^{-\mathrm{i}\nu_n0^+}\Big[K_{i,j}^{(+3)}(z,\nu_n) - \Big(K_{i,j}^{(+3)}(z,-\nu_n)\Big)^*\Big], \tag{C·15}$$
$$K_{i,j}^{(33)}(\nu_n) = \mathrm{i}K_{i,j}^{(+-)}(-\nu_n). \tag{C·16}$$

The function $K^{(+-)}$ is derived as follows. Because the inverse of $K^{(+-)}$ is given by $K^{(+-)-1} = (K^{-1})^{11} - (K^{-1})^{12}$, $K^{(+-)}$ satisfies the following equation,

$$\sum_j\Big[\delta_{i,j}\mu_i\frac{\mathrm{d}^2}{\mathrm{d}t^2} - \frac{1}{\mu+\sum_i\mu_i}\mu_i\mu_j\frac{\mathrm{d}^2}{\mathrm{d}t^2} + \mu_i\omega_i^2\delta_{i,j}\Big]$$
$$\times K_{j,k}^{(+-)}(t,t') = \delta(t-t')\delta_{i,k}. \tag{C·17}$$

By performing Laplace transformation, we have

$$C_{i,j}(z)K_{j,k}^{(+-)}(z) = \delta_{i,k}, \tag{C·18}$$
$$(C(z))_{i,j} = \mu_i(z^2+\omega_i^2)\delta_{i,j} - \frac{z^2\mu_i\mu_j}{\mu'}. \tag{C·19}$$

The inverse of $C(z)$, i.e. $K^{(+-)}(z)$ is expanded as

$$C^{-1}(z) = \Big[\sum_{n=0}^{\infty}(-C_1^{-1}C_2)^n\Big]C_1^{-1}, \tag{C·20}$$

where $(C_1)_{i,j} = \mu_i(z^2+\omega_i^2)$ and $(C_2)_{i,j} = -z^2\mu_i\mu_j/\mu'$. From the relation $C_2(C_1^{-1}C_2)^n = \{-\sum_k\alpha_k\mu_kz^2/[\mu'(z^2+\omega_k^2)]\}^nC_2$ and $(C_1^{-1}C_2C_1^{-1})_{i,j} = -z^2/[\mu'(\omega_i^2+z^2)(\omega_j^2+z^2)]$, $K^{(+-)}(z) = C^{-1}(z)$ is given by

$$(K_{i,j}^{(+-)})_{i,j} = (C_1^{-1})_{i,j} + \frac{z^2}{\mu' - \sum_i\dfrac{\mu_iz^2}{\omega_i^2+z^2}}\cdot\frac{1}{(\omega_i^2+z^2)(\omega_j^2+z^2)}. \tag{C·21}$$

With the use of $r_i = \mu_i/\mu'$, we obtain

$$\sum_{i,j} r_iK_{i,j}^{(+-)}(z)r_j = \frac{1}{z^2}\left(-\frac{1}{\mu'} + \frac{1}{\mu + \sum_i\dfrac{\mu_i\omega_i^2}{\omega_i^2+z^2}}\right). \tag{C·22}$$

We rewrite eq. (C·22) as $-G_0^{(+-)}(z) + K_0^{(+-)}(z)$ where $G_0^{(+-)}(z) \equiv 1/(\mu'z^2)$ and $K_0^{(+-)} = 1/\{z^2[\mu + \sum_i\mu_i\omega_i^2/(\omega_i^2+z^2)]\}$. By using the relations eqs. (C·14), (C·15) and (C·16) this expression is applied to the other components as $\sum_{i,j} r_iK_{i,j}^{(l,m)}r_j = -G_0^{(lm)} + K_0^{(lm)}$, where $(l,m) = (+,+)$, $(+,3)$, and $(3,3)$. The functions $G_0^{(l,m)}$ and $K_0^{(l,m)}$ also satisfy the relation eqs. (C·14), (C·15) and (C·16). From these relations, $G_0^{(l,m)}(t,t')$ is given by eq. (3.14). Then eq. (C·10) is written as eqs. (3.12), (3.13) and (3.15).

By introducing the spectral density $I(\omega)$, the inverse Laplace transformation of the function $K_0^{(+-)}(z)$ in the case of the Gaussian–Markovian dissipation is reduced to eq. (3.20). From the relation eq. (C·15), $K_0^{(++)}(z)$ in the Gaussian–Markovian dissipation case is given by

$$K_0^{(++)}(z) = \sum_{l=1}^{\infty}\frac{2\mathrm{i}\gamma\omega_D^2}{\beta\hbar\mu\nu_l(z+\nu_l)[(\nu_l^2+\gamma\omega_D)^2 - \nu_l^2\omega_D^2]}$$
$$+ \sum_{l=1}^{\infty}\frac{\mathrm{i}}{\beta\hbar\mu(x_1-x_2)}\left[\frac{2x_2}{(z+x_2)(x_2^2-\nu_l^2)}\left(1-\frac{x_1}{\gamma}\right)\right.$$
$$\left.- \frac{2x_1}{(z+x_1)(x_1^2-\nu_l^2)}\left(1-\frac{x_2}{\gamma}\right)\right]$$
$$+ \lim_{l\to0}\frac{\mathrm{i}\mathrm{e}^{-\mathrm{i}\omega_l0^+}}{\beta\hbar\mu z(\nu_l^2 + |\nu_l|\hat{\gamma}(|\nu_l|))}$$
$$- \frac{\mathrm{i}}{\hbar\beta\mu}\left\{\frac{1}{x_1-x_2}\left[\left(1-\frac{x_2}{\gamma}\right)\frac{1}{x_1(z+x_1)}\right.\right.$$
$$\left.- \left(1-\frac{x_1}{\gamma}\right)\frac{1}{x_2(z+x_2)}\right]$$
$$\left.+ \frac{1}{\gamma\omega_Dz}\left(1-\frac{\omega_D}{\gamma}\right) + \frac{1}{\gamma z^2}\right\}, \tag{C·23}$$

where $x_{1,2}$ is defined by eq. (3.24). Performing the inverse Laplace transformation, we obtain $K_0^{(++)}(t)$ given in eq. (3.21). Similarly, we can obtain $K_0^{(+3)}(t,\tau)$ and $K_0^{(33)}(\tau)$ given by eqs. (3.22) and (3.23) by using the relation (C·15) and

(C·16), respectively.

1) P. Debye: *Polar Molecules* (Reinhold Publishing, New York, 1929).
2) *Molecular Spectroscopy*, ed. D. A. Long, D. J. Millen and R. F. Barrow (Chemical Society, London, 1974) Vol. 2.
3) W. G. Rothschild: *Dynamics of Molecular Liquids* (John Wiley, New York, 1984).
4) H. Katsuki and T. Momose: Phys. Rev. Lett. **84** (2000) 3286.
5) N. Neumann: J. Chem. Phys. **82** (1985) 5663; *ibid.* **85** (1986) 1567.
6) L. E. Bowman, B. J. Palmer, B. C. Garrett, J. L. Fulton, C. R. Yonker, D. M. Pfund and S. L. Wallen: J. Phys. Chem. **100** (1996) 18327.
7) N. Yoshii, H. Yoshie, S. Miura and S. Okazaki: J. Chem. Phys. **109** (1998) 4873.
8) J. Jang and R. M. Stratt: J. Chem. Phys. **113** (2000) 5901; *ibid.* **113** (2000) 11212.
9) A. O. Caldeira and A. J. Leggett: Physica A **121** (1983) 587; *ibid.* **130** (1985) 374(E).
10) H. Grabert, P. Schramm and G.-L. Ingold: Phys. Rep. **168** (1988) 115.
11) P. Hänggi, P. Talkner and M Borkovec: Rev. Mod. Phys. **62** (1990) 745.
12) U. Weiss: *Quantum Dissipative Systems* (World Scientific, Singapore, 1999) 2nd ed.
13) A. I. Burshtein and S. I. Temkin: *Spectroscopy of Molecular Rotation in Gases and Liquids* (Cambridge University Press, Cambridge, 1994).
14) A. P. Kouzov: Phys. Rev. A **60** (1999) 2931.
15) J. E. Hunter III, D. G. Taylor III and H. L. Strauss: J. Chem. Phys. **97** (1992) 50.
16) W. Dittrich and M. Reuter: *Classical and Quantum Dynamics Form Classical Paths to Path Integrals* (Springer, Berlin, 1994) 2nd ed.
17) J. Cao: Phys. Rev. E **49** (1994) 882.
18) Y. Suzuki and Y. Tanimura: J. Phys. Soc. Jpn. **70** (2001) 1167.
19) S. Mukamel: *Principle of Nonlinear Optical Spectroscopy* (Oxford, New York, 1995).
20) R. Fukuda, M. Sumino and K. Nomoto: Phys. Rev. A **45** (1992) 3559.
21) R. Fukuda, M. Komachiya, S. Yokojima, Y. Suzuki, K. Okumura and T. Inagaki: Prog. Theor. Phys. Suppl. No. 121 (1995) 1.
22) V. Hakim and V. Ambegaokar: Phys. Rev. A **32** (1985) 423.
23) Y. Tanimura and R. Kubo: J. Phys. Soc. Jpn. **58** (1989) 101.
24) Y. Tanimura and P. G. Wolyness: Phys. Rev. A **43** (1991) 4143; J. Chem. Phys. **96** (1992) 8485.
25) R. P. Feynman and A. R. Hibbs: *Quantum Mechanics and Path Integrals* (MacGraw-Hill, New York, 1965).
26) C. Uchiyama and F. Shibata: Physica A **153** (1988) 469.
27) C. Uchiyama and F. Shibata: Physica A **161** (1989) 23.
28) Y. Suzuki and Y. Tanimura: Chem. Phys. Lett. **358** (2002) 51.